Performance Evaluation of a Simplified Multi-Function Current Transformer for High Frequency Power Converters

D C Pentz
Group on Electronic Energy Processing
University of Johannesburg
Johannesburg, South Africa
davidp@uj.ac.za

F H van der Merwe
Imfuyo Projects (Pty) Ltd
Benoni, South Africa
fvdmerwe@gmail.com

Abstract— **A multi-function current transformer introduced some years ago is revisited in an effort to improve its manufacturability. The original current sensor has the ability to accurately represent load and phase-arm currents in single phase full-bridge dc-dc-converter topologies under normal operating conditions. In the event of a phase-arm fault the shoot-through current can also be detected and the information used in the protection scheme. This sensor is however very complex to manufacture and this work presents a simplified version of the sensor, which still gives the most important information with a far less complex structure. This paper briefly discusses the original current sensor, proposes a simplified sensor and evaluates the new sensor in terms of performance.**

Keywords-current transformer; current sensor; power electronic converter

I. INTRODUCTION

Accurate current sensing has always been a very important aspect in the field of electrical engineering [1]. Current waveforms in high frequency power converters contain valuable information about the operation of a converter [2], [3]. Good load current regulation and effective protection schemes also rely heavily on the quality of the current sensor output. Integration of multiple functions into single devices also helps reduce size and cost of converters [4].

Several types of current sensors have been developed over the years. Resistive current sensing is probably one of the simplest methods used but lacks galvanic isolation [4]. Coaxial shunts offer very good noise immunity and the low inductance increases their bandwidth [5], [6]. Hall-effect sensors have gained popularity in recent years because of the reduction in cost and their ability to measure dc- and ac-currents but bandwidth still limits the amount of obtainable waveform detail [4] and offsets may occur due to temperature variation [7]. Other current sensors such as Rogowski coils and giant magneto-resistive current sensors are also discussed in [4]. A good overview of current sensing technologies is discussed in [4], with the emphasis on the ability to integrate these sensors. Current transformers (CT) are still very popular because of the ease with which they can be designed and manufactured for a specific current range and large bandwidth [4]. Additional driver circuits are not required and they consume very little power [8]. CT's do however introduce some inductance in the current path but this is a problem generally experienced with current sensors. The inability of a current transformer to measure a current waveform with a constant dc-component is the main draw-back of this technology. In a pulsed dc-current application, care should be taken in the design to ensure that the CT-core does not saturate [8]. In [9] several current transformer configurations are listed for single-phase, full-bridge topology applications. The integrated current sensor proposed in [9] will be discussed briefly in the next section. This paper is aimed at proposing an alternative current transformer with a reduced structural complexity, but with the same functionality as the integrated current sensor proposed in [9].

II. INTEGRATED CT

A. Complex current sensor previously proposed

In this section the sensor proposed in [9] is briefly discussed to give the reader the required background.

Usually, in isolated dc-dc converters of class-E type, the load current needs to be regulated or monitored for over-current conditions. Current transformers are then often used to measure the ac-current in the load path. If one of the switches or drivers in the bridge-topology however fails due to one of a number of possible reasons, the other device in the same phase-arm and the rest of the bridge need to be protected against the resulting short-circuit currents which can be substantial due to the energy stored in the dc-bus capacitors. The CT in the load path is incapable of detecting this type of fault. The stray inductance in these parts of the topology is deliberately minimized and thus a current sensor and the signal conditioning electronics with good response are

required because of the fast rise times of the fault current. Many designers simply insert shunt resistors or Hall-effect current transducers below the low side switches to sense the pulsed dc-current in the phase arm and ensure that fault conditions of this nature are detected. The drain-source resistance of MOSFET's can also be used for this purpose [10] but the ever decreasing on-resistance of these devices result in relatively low voltages that have to be filtered and amplified carefully to obtain realistic information.

Refer to figure 1 for the complex current sensor proposed earlier and the flux patterns set up during the first switching and freewheeling cycles. This yields insight to the operation of the device. An EE-core with multi-turn secondary windings on the centre and outer legs is positioned in a full-bridge topology as shown in figure 1. Five single turn primary windings are wound through the current transformer as shown. The principle is that, under normal operating conditions the diagonal switch currents cause flux in the outer legs of the EE-core that oppose each other and only the load current is measured via secondary winding N_{s2} positioned on the centre leg of the CT. If a fault occurs where both switches in a phase arm switch on simultaneously, current will flow through the top and bottom primaries of the corresponding phase-arm and flux the core in the same direction. No current will flow through the load or through the opposite phase-arm primaries and the only current measured will be the fault current. The secondary windings on the outer legs may be connected to detection circuitry individually or in a differential manner and the faulty phase-arm may then be identified. With the secondary windings connected as shown in figure 2 the differential output of the secondary windings in those paths should be zero (provided that the windings are perfectly symmetric) and the load current alone causes a volt drop across the burden resistor R_B.

A simplified reluctance model of this current sensor is presented in figure 3. In this figure, $\Im$ represents mmf, $\Re$ is

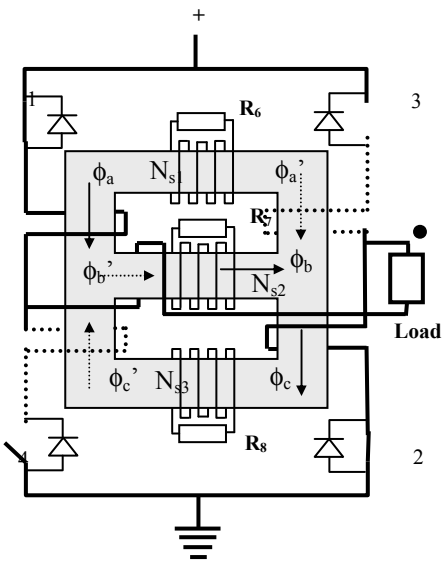

Figure 1. Complex integrated current sensor

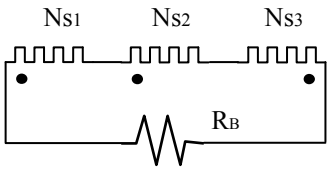

Figure 2. One possible secondary winding connection

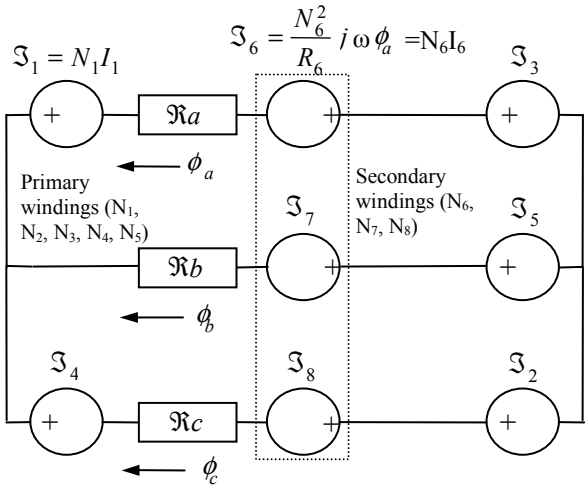

Figure 3. Simplified reluctance model

reluctance, ϕ equals flux, N is the number of turns per secondary winding and R the value of the burden resistance for each of the secondary windings. This analysis is performed in [9], where the circuit equations (1), (2), (3) and (4) obtained through a mesh-current analysis technique are solved symbolically for the flux in each leg of the core.

$$\Im_1 + \Im_3 - \Im_5 - \Im_6 + \Im_7 = \phi_a \Re_a \quad (1)$$

$$\Im_2 + \Im_4 - \Im_5 + \Im_7 - \Im_8 = -\phi_b \Re_b + \phi_c \Re_c \quad (2)$$

$$\Im_1 - \Im_2 + \Im_3 - \Im_4 - \Im_6 + \Im_8 = \phi_a \Re_a - \phi_c \Re_c \quad (3)$$

$$\phi_a + \phi_b + \phi_c = 0 \quad (4)$$

During normal operating conditions symmetry in the circuit allows some simplification eg. $\Im_1 = \Im_2$, $N_6 = N_7 = N_8$, $\phi_a = \phi_c$ etc. The equations, containing complex numbers are solved with MATLAB. Neglecting all leakage components and assuming zero reluctance for the material yields the following results. The output voltage of each secondary winding in terms of the load current i_L, terminating resistance R=22Ω, number of secondary turns N_S=88 and number of primary turns N_P=1, is given by equations (5) and (6) [9].

$$v_6 = v_8 = 0.67 N_p i_L R_6 / N_s = i_L / 6 \quad (5)$$

$$v_7 = 1.33 N_p R_7 i_L / N_7 = i_L / 3 \quad (6)$$

The experimental verification of these equations is presented in [9] but it is also repeated in section III so that it may be compared with the new results. The normal operating

current as well as load and phase-arm fault conditions are successfully captured by the CT [9].

The construction of this current sensor is also fairly complex, as shown in the next section, because three secondary windings need to be fitted onto the same core. Special bobbins are required for the outer legs as their areas are half the centre leg area. Connections have to be done by hand, impacting on the cost, and the primary windings need to be connected carefully so that proper operation is ensured. These problems were addressed partially by using a printed circuit board as the basis for constructing the converter circuit with the current sensor.

B. Simplified current sensor

A new sensor layout is now proposed in figure 4. This current transformer has only one secondary winding and two primary windings. Now trace the current paths during normal operation. For the first half cycle, current flows through the first primary winding and bypasses the core through the load to the low-side switch on the right hand side of the bridge. For the second half cycle the current flows through the second primary winding in such a way that the flux direction in the centre leg of the core is reversed and the secondary current is thus proportional to the load current while the core is reset.

The core experiences ac-flux excursions only as long as the bridge is operated with a symmetrical duty cycle, a condition normally required for isolated dc-dc-converters. The secondary winding output represents the load current under these conditions and can be used for current regulation or current limiting purposes. Fault conditions on the load side, before or after rectification, can be detected by monitoring and responding to corresponding increases in the output voltage of the current sensor. The polarity of the output voltage can be used to identify the faulty phase-arm, should this information be required. In case of a phase-arm experiencing shoot-through the load is bypassed and the current flowing in either of the primary windings will cause the output voltage across the burden resistor to rise proportionally to the fault current. External circuitry responsible for fault detection and protection should respond rapidly to such a condition and prevent any further switch operation.

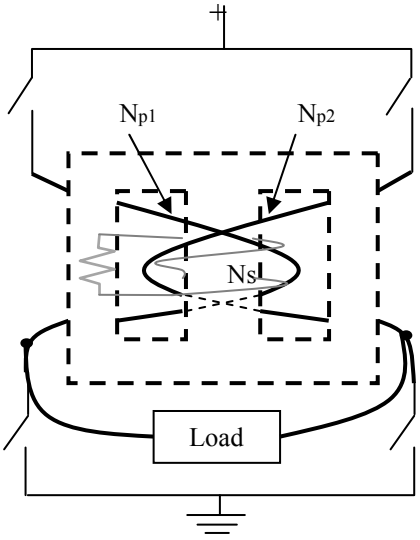

Figure 4. Simplified integrated current sensor

The analysis of this current transformer is much simpler than the complex sensor discussed in the previous section since the secondary current is directly proportional to the primary current all the time.

III. EXPERIMENTAL VERIFICATION

Figure 5 shows photographs of the physical current sensors discussed in this paper, clearly illustrating the simplification of the newly proposed arrangement. Unlike the complex CT arrangement discussed earlier, the measured current for the simplified integrated CT is simply calculated as a function of the turns ratio, the value of the burden resistance and the voltage measured across it. The construction is also simplified and no special bobbins are needed since the secondary is wound on the bobbins designed for standard EE-core arrangements. The complexity of the conditioning circuitry required is also reduced because all the information is obtained via a single burden resistor.

Some results of the original current sensor are now shown first and then the results of the newly proposed sensor are presented.

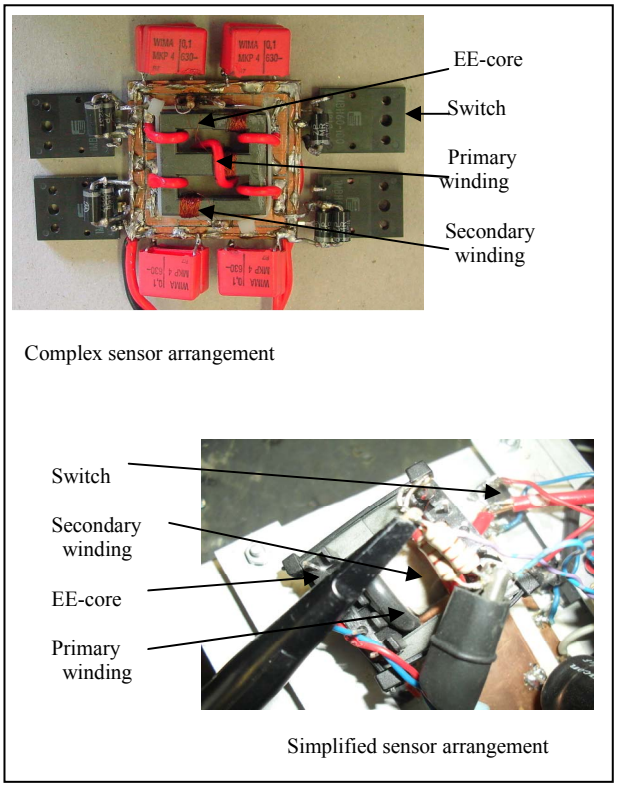

Figure 5. Photographs

A. *Waveforms obtained with complex current sensor previously proposed*

The waveforms presented in figure 6 are for normal operation of the converter. The secondary output voltage for a 8A(peak) actual load current should be approximately 2.7V according to equation (6) from the reluctance model. The measured output voltage is approximately 2.5V. The waveform measured with the CT correlates with the actual current very well apart from the droop. Differences between the expected and actual values may be attributed to the droop and the assumptions made in the analysis.

Figure 7 shows results with a non-symmetrical duty cycle resulting in the expected elimination of the dc-offset.

This CT allowed the protection circuit to disable the converter in under 1µs from the moment the current exceeds the reference value as indicated in figure 8.

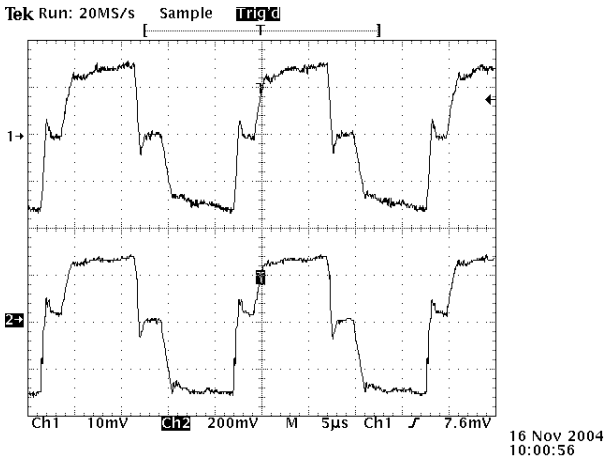

Figure 6. Waveforms under normal operating conditions
CH1 Actual load current (5A/div)
CH2 Secondary output voltage V_7 (2V/div)

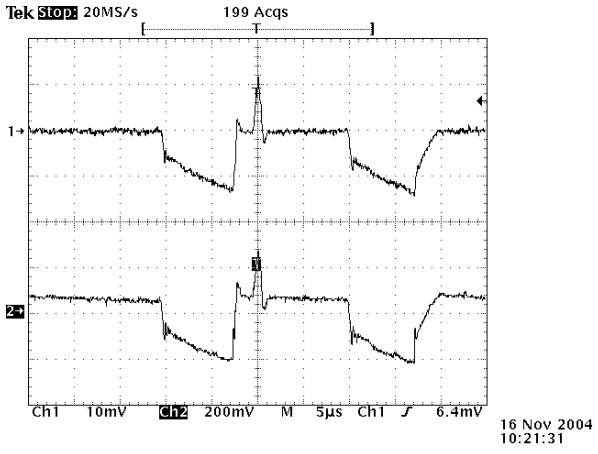

Figure 7. CH1 Actual load current (5A/div)
CH2 Secondary output voltage V_7 with current limiting causing a non-symmetrical load current. (2V/div)

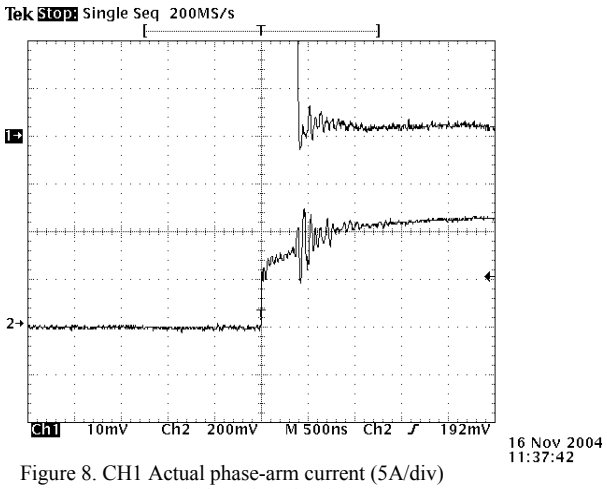

Figure 8. CH1 Actual phase-arm current (5A/div)
CH2 Fault detection circuit output responsible for resetting the circuit. (2V/div)

B. *Waveforms obtained with simplified current sensor*

Waveforms measured with a good quality current probe and amplifier (Tektronix TCP312 and TCPA300) are shown with the output voltage of the simplified current sensor for a few cases. Firstly the waveforms under normal operating conditions and symmetrical duty cycle are shown in figure 9. The peak switch current is approximately 1A, which is consistent with the 10V load voltage across a 10Ω wire wound resistor. The waveform of the CT output voltage is very similar in appearance. The turns ration Np:Ns is 1:600 and the value of the burden resistor is 108Ω measured cold. The 106mV peak value of the CT output thus translates into a load current of 0.9A. If the duty cycle is not balanced the waveforms still appear to be very similar but the dc-offset is eliminated by the CT as expected. These waveforms are not shown here.

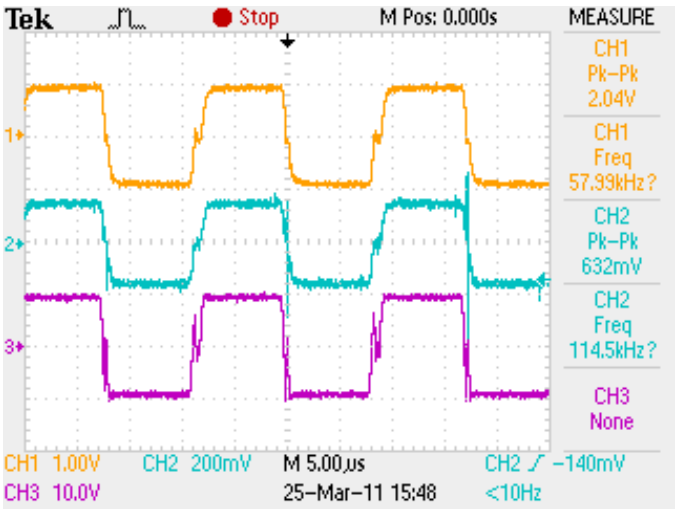

Figure 9. Waveforms under normal operating conditions
CH1 (1V/div): Actual load current (1A/V)
CH2 (200mV/div): CT output voltage
CH3 (10V/div): Load voltage

Next, a fault is simulated by connecting a low resistance in parallel with the load resistor because no protection scheme is yet employed in the control circuit. The current in the load path increases to a value of 4A and the current measured by the CT is approximately 3.8A as shown in figure 10. The load voltage does not drop to zero as would be expected in the case of a proper short-circuit condition across the load.

If one of the switches in the converter is shorted, the phase arm fault current measured with the current probe and CT are 9A and 8.8A respectively. The power supply feeding the circuit is current limited because no shutdown strategy is employed in this part of the experimental setup. The majority of the fault current is however expected to be sourced from the dc-bus capacitance directly after the fault occurs and therefore the bus capacitance is also reduced for experimental purposes. The load voltage is zero for the faulty half cycle since no current flows in the load. The CT output voltage represents the load current up to the point where the fault is introduced and then it represents the fault current. It immediately starts to eliminate the dc-offset as expected. The waveforms are shown in figure 11.

With full protection schemes employed the converter may be forced into a fault condition repeatedly. The CT provides accurate fault information which enables the protection circuit to disable the converter safely within less that 1µs from the moment the current exceeds the set value. These results are not shown in this article but are very similar to the results shown in figure 8 [9].

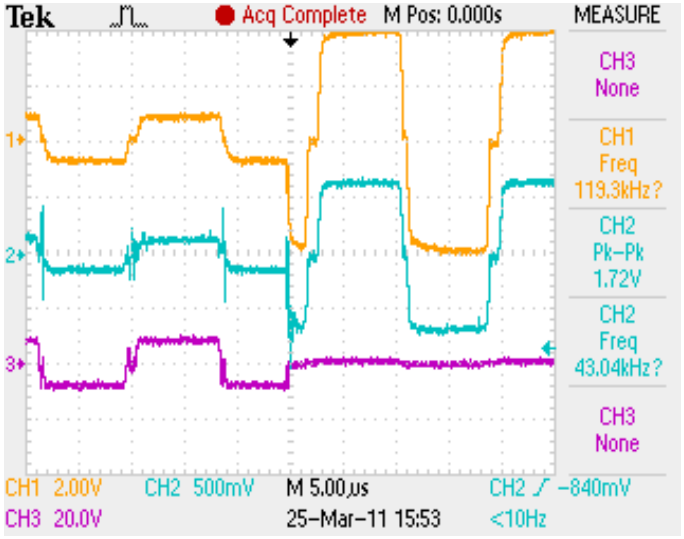

Figure 10. Waveforms with load short circuit
CH1 (2V/div): Actual load current (1A/V)
CH2 (500mV/div): CT output voltage
CH3 (20V/div): Load voltage

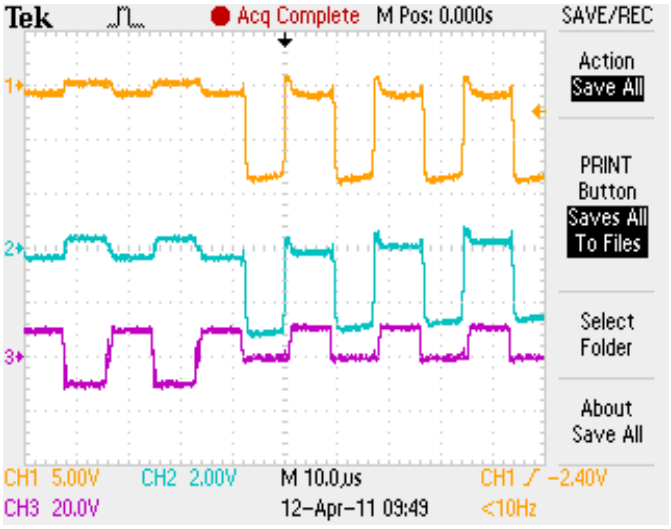

Figure 11. Waveforms with phase arm short fault
CH1 (5V/div): Actual phase arm current (1A/V)
CH2 (2V/div): CT output voltage
CH3 (20V/div): Load voltage

IV. CONCLUSION

This work successfully demonstrates the functionality of the newly proposed integrated current sensor arrangement. Both the analysis and the construction of this sensor are shown to be much simpler than the previously proposed solution. The current waveforms measured with the CT are very similar to the ones obtained using a current probe and for cases where the duty cycle symmetry is disturbed, the CT eliminates the dc-component as expected. The only waveforms that cannot be obtained readily are the individual phase arm currents.

REFERENCES

[1] D. A. Douglass, "Current Transformer Accuracy with Asymmetric and High Frequency Fault Currents.", *IEEE Transactions on Power Apparatus and Systems*, vol. PAS-I00, no. 3, March 1981.

[2] D. Y. Qiu, S. C. Yip, Henry Shu-Hung Chung, and S. Y. Ron Hui, "On the Use of Current Sensors for the Control of Power Converters.", *IEEE Trans on Power Electronics*, vol. 18, no. 4, July 2003.

[3] N. Mc Neill, N. K. Gupta and W. G. Armstrong, "Active current transformer circuits for low distortion sensing in switched mode power converters" *IEEE Trans on Power Electronics*, Vol. 19, No. 4, pp 908-917.

[4] E. Laboure, F. Costa and F. Forest, " Current measurement in static converters and realization of a high frequency passive current probe (50 A-300 MHz)", *Fifth European Conference on Power Electronics and Applications*, Sept 1993, vol. 4, pp. 478 -483.

[5] J. A. Ferreira, W. A. Cronje and W. A. Relihan, **"**Integration of high frequency current shunts in power electronic circuits," *IEEE Transactions on Power Electronics*, vol. 10, No. 1, pp. 32 – 37, 1995.

[6] Y. Xu and R. D. Lorenz, "Design of integrated shunt current sensors for IPEMs," *Proc. of CPES Seminar 2002*, pp. 404-411, 2002.

[7] J. Trontelj**,** "Optimization of integrated magnetic sensor by mixedsignal processing," *Proceedings of the 16th IEEE Instrumentation and Measurement Technology Conference*, vol. 1, pp. 299–302, 1999.

[8] Chucheng Xiao, Lingyin Zhao, Tadashi Asada, W. G. Odendaal and J. D. van Wyk, “An overview of Integratable Current Sensor Technologies.”, *Proceedings of IAS 2003*.

[9] D. C. Pentz and I. W. Hofsajer, “Performance Evaluation of a Novel Integrated Current Sensor in High Power Isolated Power Converters”, *Proceedings of SAUPEC 2005*.

[10] Yang Zhang, Zane, R, A. Prodic, R. Erickson and D. Maksimovic, “Online calibration of MOSFET on-state resistance for precise current sensing**”,** *Power Electronics Letters, IEEE,* vol. 2, Issue 3, Sept. 2004, pp 100 – 103.